

Electron Dynamics in Copper Metallic Nanoparticles Probed with Femtosecond Optical Pulses

J.-Y. Bigot, J.-C. Merle, O. Cregut, and A. Daunois

Institut de Physique et Chimie des Matériaux de Strasbourg, Groupe d'Optique Nonlinéaire et d'Optoélectronique, Unité mixte 380046 CNRS-ULP-EHICS, 23 rue du Loess, 67037 Strasbourg Cedex, France

(Received 9 May 1995)

The thermalization of electrons in copper nanoparticles embedded in glass is investigated using femtosecond pump-probe spectroscopy. The time dependent induced transmission is enhanced near the surface plasmon resonance of the nanoparticles, as opposed to the static one obtained with thermomodulation measurements. In addition, a slowing of the process of electron cooling to the lattice temperature is observed at the plasmon resonance. These observations show the importance of quasiparticle collisions in confined metallic structures.

PACS numbers: 78.47.+p

The scattering and absorption of light by metallic nanoparticles embedded in a transparent matrix depend on both the complex dielectric function of the metal and the boundary conditions at the metal surface. In particular, in the spectral region corresponding to the first order plasmon mode obtained from the theory of Mie [1], the optical susceptibility is resonantly enhanced [2]. Regarding the electron dynamics in metal spheres, the surface scattering of electrons leads to a linewidth of the plasma resonance inversely proportional to the particle size. It can be taken into account by an effective mean free path of electrons propagating at the Fermi velocity [3–5]. This geometrical effect is, *a priori*, not related to the thermodynamics of the electron distribution. The aim of the present work is to investigate the dynamics of hot electrons in copper spheres when a nonequilibrium quasiparticle population is created by ultrashort optical pulses. The dominant scattering processes involved in this temporal domain are electron-electron (*e-e*) and electron-phonon (*e-p*) collisions. Unique information on the dynamics of metallic confined structures is obtained by comparison with measurements in thin metal films.

The dynamics of the electron gas in the nanoparticles is investigated with femtosecond pump-probe spectroscopy as reported in the study of metal films [6–8]. The pump pulse initially heats the electron gas which subsequent thermalization and relaxation to the lattice is temporally and spectrally resolved with the probe pulse. Thermalization refers here to the temporal regime during which *e-e* collisions are very effective in redistributing the initial nonequilibrium quasiparticle distribution. An important aspect in the case of copper spheres is the transition $d \rightarrow E_F$ from the filled *d* band to the Fermi level of copper (energy E_F) and the plasmon resonance which energy E_{plasmon} is close to this transition. Two main results are reported. First, the time dependent transmission spectra are compared with those obtained with a static thermomodulation technique on the same sample. These measurements show that the differential transmission is enhanced near the plasmon resonance during several hundred femtoseconds. This confirms the results of Fann *et al.* [9] who have shown that in

gold films the initial non-Fermi-Dirac electronic distribution persists for a very long time (~ 1 ps) after excitation. It clearly establishes that the electron dynamics in metal nanoparticles must include *e-e* interactions and not only the energy relaxation to the lattice, as recently proposed in a similar system [10]. Second, the relaxation of electrons to the lattice is slower at the surface plasmon resonance. This effect is absent in copper films in the same energy range. A Landau damping mechanism is proposed to explain this process.

For the femtosecond pump probe experiment, we use pump pulses of 80 fs duration generated by a 620 nm colliding pulse mode-locked cavity, amplified by a 5 kHz copper-vapor laser. The probe pulses of 10 fs duration come from a fiber-generated, third-order-compensated continuum using part of the amplified beam [11]. The maximum pump energy density is 0.5 mJ cm^{-2} corresponding to a rise of the electronic temperature of several hundred kelvin. The differential transmission spectra $\Delta T/T(\hbar\omega, t)$ are measured with a spectrograph and dual-array multichannel analyzer as a function of the time delay *t* between the pump and probe pulses. For the static thermomodulation experiments, we use the 488 nm line of a cw argon laser as a heating source and a stabilized tungsten lamp as the probe. The 200 mW unfocused pump beam corresponds to a sample heating of a few kelvin. The same detection is used to measure the static thermomodulation spectra $\Delta T_{\text{stat}}/T$. The samples are copper nanoparticles with spherical shape of 10 nm diameter as measured by transmission electron microscopy. They are embedded in a 150- μm -thick glass matrix with a volumic concentration of 2×10^{-4} , so that interparticle effects can be neglected. In addition, we compare the dynamics obtained in the spheres with the one obtained from copper films. We use 30-nm-thick polycrystalline films freshly deposited on a glass substrate. All the measurements are performed at room temperature.

Figure 1(a) shows the optical density of the sample containing the nanoparticles, the pump and probe spectra, and the spectral positions of the plasmon resonance and $d \rightarrow E_F$ transition. The choice of copper as the active

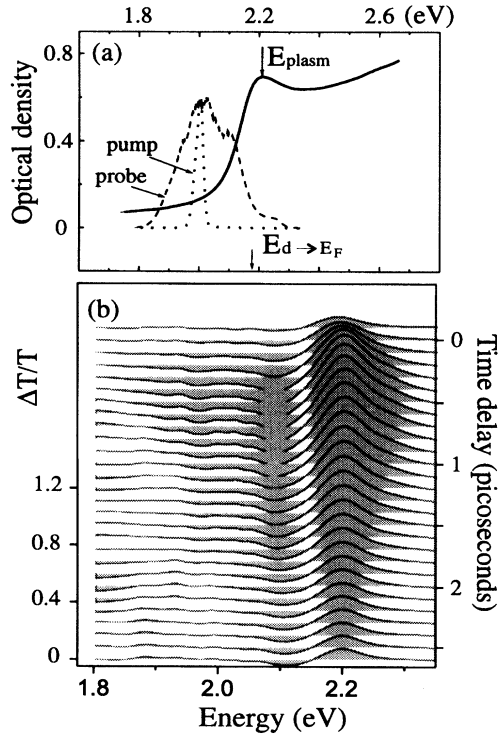


FIG. 1. (a) Absorption spectrum (full line) of the copper nanoparticle sample near the Mie resonance and spectra of the pump (dotted) and probe (dashed) pulses. (b) Pump-probe differential transmittance from the copper nanoparticles with 0.5 mJ/cm^2 pump intensity.

metal is determined by the proximity of these two energies, which is an important requirement for the present study. ($E_{dF} \approx 2.19 \text{ eV}$, $E_{\text{plasm}} \approx 2.22 \text{ eV}$). In Fig. 1(b), the differential transmission $\Delta T/T(\hbar\omega, t)$ is represented for various pump-probe delays. This series of spectra shows the overall electron redistribution around the Fermi level ($\Delta T/T > 0$ or < 0 correspond to occupied or empty states, respectively). Initially and during about 700 fs, the spectra broaden on both sides of the Fermi level and narrow later on during the *cooling* process. Another important feature is the asymmetric spectral shape of $\Delta T/T$ with respect to the energy crossing point ($\Delta T/T = 0$), which is observed during the first picosecond. This is better seen in Fig. 2(a) where we have plotted $\Delta T/T$ for the delay 0.5 ps (dashed line) together with the static thermomodulation signal $\Delta T_{\text{stat}}/T(\hbar\omega)$ (full line). While $\Delta T_{\text{stat}}/T(\hbar\omega)$ has comparable positive and negative contributions, $\Delta T/T(\hbar\omega, t = 0.5 \text{ ps})$ is enhanced in the energy range close to the plasmon resonance. This behavior is proper to the nanoparticles. In the case of the thin copper films, the dynamical and static measurements both present the same spectral features in transmission as well as in reflectivity. Note that for the glass embedded particles the very weak differential reflectivity spectra ($\Delta R/R \approx 10^{-5}$) do not affect the transmission measurements.

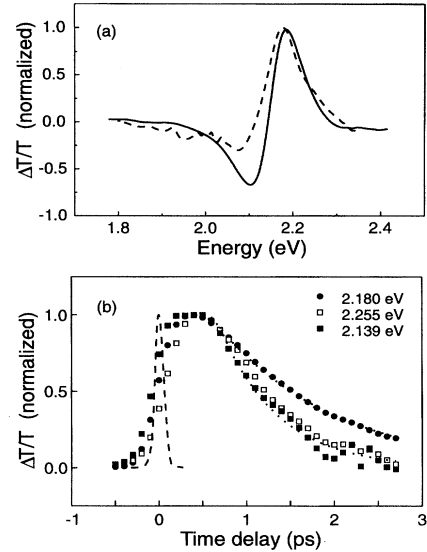


FIG. 2. (a) Spectral shapes of the differential transmittance spectra from the copper nanoparticles: static cw excitation (full line), pulsed excitation with 500 fs pump-probe delay (dashed line). (b) Temporal evolution of the pump-probe signal for different probe photon energies near E_{plasm} .

Figure 2(b) shows temporal cross sections of $\Delta T/T$ for different energies $\hbar\omega = 2.255, 2.18, \text{ and } 2.139 \text{ eV}$. It is seen that the decay time is longer near the resonance. The dotted curves correspond to exponential decays of 1.3 ps (at 2.18 eV) and 700 fs off resonance. This suggests a relaxation mechanism that is related to the small size particles. In contrast, in the case of thin films, the dynamics is identical over the entire energy range around the $d \rightarrow E_F$ transition as reported by El-Sayed *et al.* [7]. This was also checked with our 30 nm copper films. The relaxation time is then comprised between 800 and 900 fs over the energy range 2.22–2.06 eV. The dashed curve in Fig. 2(b) represents the cross correlation of the 80 fs heating pulse with the 10 fs probe pulse, measured with a KDP crystal. An important temporal delay is observed between the pulse and the maximum of the signal.

We now investigate the importance of $e-e$ and $e-p$ scatterings on the observed dynamics. The dielectric function of copper is modeled with collective modes via a Drude-like intraband term ϵ_{intra} and quasiparticle states with distribution $\mathcal{F}(\hbar\omega, \Theta)$ at temperature Θ via an interband term ϵ_{inter} . Depending on the excitation regime, Θ represents either the lattice temperature Θ_1 or the electronic temperature $\Theta_e(t)$. Within the random phase approximation (RPA), one obtains [12]

$$\epsilon_{\text{intra}} = 1 - \frac{\Omega_{p,\text{eff}}^2}{\omega(\omega + i\hbar\gamma_{\text{eff}})}, \quad (1)$$

$$\epsilon_{\text{inter}} = K \int_0^\infty dx \frac{\sqrt{\hbar x - E_g}}{x} \times [1 - \mathcal{F}(x, \Theta)] \frac{(\omega^2 - x^2 - \gamma_{ee}^2 - 2i\omega\gamma_{ee})}{(\omega^2 - x^2 - \gamma_{ee}^2)^2 + 4\omega^2\gamma_{ee}^2}, \quad (2)$$

where $\Omega_{p,\text{eff}}$ and γ_{eff} are the effective plasma frequency and inverse collision time of the collective mode, taking into account the surface scattering of the electrons at the metal-glass interface. They can be derived within a quantum description of the confined electronic states in the sphere [4,13]. For the interband term, we assume a dispersionless d band and a parabolic conduction band with mass m^* and minimum energy $E_g = \hbar\omega_g$ with respect to the d band. γ_{ee} is the inverse scattering time between quasiparticles. The constant K is equal to $8\mu^2 e^2 m^* \sqrt{2m^*} / \pi \hbar^3 m^2$, where μ is the dipole moment which is supposed wave vector independent for all transitions and obtained from the f -sum rule.

Equations (1) and (2), together with the Mie theory, allow one to reproduce the static thermomodulation measurements. The differential spectra are obtained via the variation of the lattice temperature Θ_L in the electron occupation number $\mathcal{F}(\hbar\omega, \Theta_L)$ and via a linear temperature dependence of the effective plasma damping ($\gamma_{\text{eff}} = \gamma_{\text{eff}}^{(0)} + \gamma_{\text{eff}}^{(1)}\Theta_L$). This procedure is analogous to the one used by Rosei and Lynch [14] to explain thermomodulation in thin copper films, except for the additional $e-e$ damping γ_{ee} in the integral of the interband dielectric function. Even though in the static regime of excitation, and at room temperature, the dominant damping mechanism is due to intraband processes via $e-p$ scattering [15], we find that a weak $e-e$ damping enables one to better fit the experimental curves. This is due to the fact that, in copper, the Debye temperature Θ_D , which determines the relative importance of $e-e$ and $e-p$ collisions, is slightly higher than the room temperature at which the experiments are performed ($\Theta_D \approx 315$ K). The glass-nanoparticle transmission is calculated using the Mie scattering coefficients a_l and b_l for the electric and magnetic modes [16] up to order $l = 5$:

$$T(\hbar\omega, \Theta_L) = \exp\left(-\frac{2\pi R^2 LN}{x_0^2} \times \sum_{l=1}^{\infty} (2l+1) \text{Re}[a_l(x_0, x_i) + b_l(x_0, x_i)]\right), \quad (3)$$

with

$$x_0 = \frac{\omega}{c} \sqrt{\varepsilon_{\text{glass}}}, \quad x_i = \frac{\omega}{c} \sqrt{\varepsilon_{\text{intra}} + \varepsilon_{\text{inter}}},$$

where R is the particle diameter, N the volume density of nanoparticles, L the sample thickness, c the speed of light, $\sqrt{\varepsilon_{\text{glass}}}$ the refractive index of the glass matrix. Figures 3(a) and 3(b) show the computed optical density and thermomodulation spectra using Eqs. (1)–(3), together with the experimental ones. $\Delta T_{\text{stat}}/T(\hbar\omega)$ corresponds to an increase of the lattice temperature $\Delta\Theta_L$ of 15 K. The parameter values are $R = 5$ nm, $L = 0.15$ mm, $\varepsilon_{\text{glass}} = 2.25$ (the weak frequency dispersion of the glass matrix being neglected), $\gamma_{ee} = 0.05$ eV, $\gamma_{\text{eff}}^{(0)} = 0.1$ eV, $\gamma_{\text{eff}}^{(1)} = 10^{-4}$ eV K $^{-1}$, $\hbar\Omega_{\text{eff}} =$

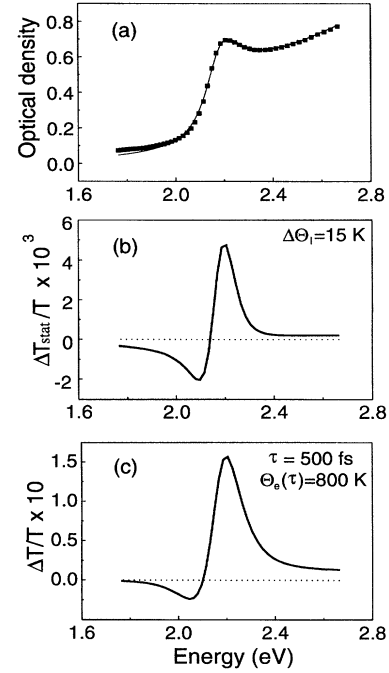


FIG. 3. Modelization of static and dynamical spectra of the copper nanoparticles: (a) fit of the linear absorption; (b) static $\Delta T/T$ corresponding to a lattice temperature elevation of 15 K; (c) dynamical $\Delta T/T$ corresponding to a pump-probe delay of 500 fs.

9.4 eV, $E_g = 1.55$ eV, and $E_F = 2.19$ eV. The above value of the plasmon damping γ_{eff} is in agreement with recent measurements on Ag islands [17] where the relaxation time of plasma oscillations is of the order of 40 fs. Introducing a size distribution in Eq. (3) we found that this fast damping process has the same spectral effects as an inhomogeneous broadening.

We now discuss the dynamical results. A first approach is to assume a time dependent electronic temperature $\Theta_e(t)$, and to compute the corresponding dielectric function for each temporal delay without considering $e-e$ scattering processes. This procedure, although employed in many works on the dynamics of thin metallic films, is not sufficient to explain the asymmetrical spectral shape of Fig. 2(a) (dotted curve). This is straightforward from Eq. (2) since, in the limit of small damping γ_{e-e} , and using $\mathcal{P}(1/x + i\gamma) = 1/x - i\pi\delta(x)$, one readily obtains

$$\frac{\partial \varepsilon_{\text{inter}}(\hbar\omega, \Theta_e)}{\partial \Theta_e} \propto -\frac{(\hbar\omega - E_F)}{k\Theta_e^2 [1 + \exp(\hbar\omega - E_F)/k\Theta_e]}. \quad (4)$$

This function has equal contributions around E_F and therefore cannot reproduce the asymmetrical spectral shapes at short delays. A more realistic approach is to introduce a damping due to $e-e$ collisions. For instance, in the Fermi liquid theory, the spectrotemporal variation

of the e - e collision time is given by [12]

$$\gamma_{ee}(\hbar\omega, \Theta_e) = \frac{(m^*)^3 \langle W \rangle}{16\pi^4 \hbar^6} \frac{(\hbar\omega - E_F)^2 + (\pi k \Theta_e)^2}{[1 + \exp(E_F - \hbar\omega)/k\Theta_e]}, \quad (5)$$

where $\langle W \rangle$ is the average transition probability for a two-quasiparticle scattering process. This formulation of the e - e scattering takes into account the Pauli exclusion near the Fermi level during the energy redistribution of the quasiparticles. In addition, one has to consider the e - p scattering as an efficient mechanism for the energy relaxation of the hot electron gas. We obtain a qualitative description of $\Delta T/T(\hbar\omega, t)$ using Eqs. (1)–(3) and (5), together with the heat equations for the electronic and lattice temperatures [18]:

$$C_e(\Theta_e) \frac{\partial \Theta_e}{\partial t} = -G(\Theta_e - \Theta_l) + P(t),$$

$$C_l \frac{\partial \Theta_l}{\partial t} = G(\Theta_e - \Theta_l), \quad (6)$$

where C_e and C_l are the electronic and lattice heat capacities, G the e - p coupling constant, and $P(t)$ the laser power density. The differential transmission is represented in Fig. 3(c) for the delay 500 fs. The parameters used are $G = 3 \times 10^{16} \text{ W m}^{-3} \text{ K}^{-1}$, $C_e = \Gamma \Theta_e$, with $\Gamma = 71 \text{ J m}^{-3} \text{ K}^{-2}$, and $C_l = 3.5 \text{ J m}^{-3} \text{ K}^{-1}$.

The above model allows one to explain the main spectral features of Fig. 2. Two temporal regimes can be distinguished. During the first one, e - e collisions are very effective, leading to the asymmetrical spectral shape $\Delta T/T$ at short delays [Fig. 3(c)]. After about 1 ps, $\Delta T/T$ becomes symmetrical as in the static case [Fig. 2(a)] which corresponds to the second regime of electronic relaxation to the lattice. The existence of the initial long-lived e - e collision regime is more and more accepted in metals [9,19,20]. We demonstrate here that it is a very important mechanism in small metal spheres. This is seen in Fig. 2(b), where the rising part of the signal is much longer than the pulse duration. Upon reaching the maximum signal, a long plateau is observed before the exponential decay takes place. Such a nonequilibrium situation cannot be described by a RPA dielectric function as used in Eq. (2). These refinements, which can be developed in the context of a many body theory, are far beyond the scope of the present Letter. In addition, the results of Fig. 2(b) show that the electron relaxation at the plasmon resonance is longer. We attribute this effect to a long lasting energy exchange between the collective excitations of the copper spheres (surface plasmon mode) and quasiparticles. This mechanism, analogous to the Landau damping in bulk materials, can prevent efficient thermalization of the electrons to the lattice temperature. Another possible mechanism is a surface trapping of the electrons at the metal-glass interface as reported in semiconductor quantum dots [21]. We leave these in-

terpretations as open questions until more theoretical and experimental work is done.

In conclusion, we have studied the electron dynamics in copper metallic nanoparticles and compared it to the one obtained in thin films. The resonant spectral features associated with the plasmon resonance of the copper spheres, show large differences as compared to lattice heating under cw laser excitation. These differences reveal the strong and long-lived electron-electron collision regime inside the nanoparticles. In addition, a slowing of the electron cooling to the lattice temperature is reported at the plasmon resonance. These results bring new information on the nonequilibrium dynamical regime of electrons in confined metallic structures.

We acknowledge interesting discussion with Pr. J. Guille on the physicochemistry of metallic nanoparticles. We are grateful to J.-L. Loison, G. Versini, and J. Werckmann for the copper nanoparticle and film characterization.

-
- [1] See, for instance, M. Born and E. Wolf, *Principles of Optics* (Pergamon Press, New York, 1959).
 - [2] J. A. Perenboom, P. Wyder, and M. Meier, *Phys. Rep.* **78**, 173 (1981); for a recent review, see C. Flytzanis *et al.*, in *Progress in Optics XXIX*, edited by E. Wolf (Elsevier, Amsterdam, 1991), p. 321.
 - [3] L. Genzel, T. P. Martin, and U. Kreibig, *Z. Phys. B* **21**, 339 (1975); U. Kreibig and C. v. Fragstein, *Z. Phys.* **224**, 307 (1969).
 - [4] A. Kawabata and R. Kubo, *J. Phys. Soc. Jpn.* **21**, 1765 (1966).
 - [5] R. Ruppin, *Phys. Rev. B* **11**, 2871 (1975).
 - [6] G. L. Eesley, *Phys. Rev. Lett.* **51**, 2140 (1983).
 - [7] H. E. Elsayed-Ali *et al.*, *Phys. Rev. Lett.* **58**, 1212 (1987).
 - [8] R. W. Schoenlein *et al.*, *Phys. Rev. Lett.* **58**, 1680 (1987).
 - [9] W. S. Fann *et al.*, *Phys. Rev. B* **46**, 13 592 (1992).
 - [10] T. Tokizaki *et al.*, *Appl. Phys. Lett.* **65**, 941 (1994).
 - [11] R. L. Fork *et al.*, *Opt. Lett.* **12**, 483 (1987).
 - [12] D. Pines and P. Nozières, *The Theory of Quantum Liquids* (W. A. Benjamin, Inc., New York, 1966), Vol. I.
 - [13] R. Ruppin and H. Yatom, *Phys. Status Solidi B* **74**, 647 (1976).
 - [14] R. Rosei and D. W. Lynch, *Phys. Rev. B* **5**, 3883 (1972).
 - [15] N. W. Ashcroft and N. D. Mermin, *Solid State Physics* (HRW International Editions, Philadelphia, 1976), Chap. 17.
 - [16] H. C. Van de Hulst, *Light Scattering by Small Particles* (Dover Publications Inc., New York, 1981).
 - [17] D. Steinmüller-Nethl *et al.*, *Phys. Rev. Lett.* **68**, 389 (1992).
 - [18] G. L. Eesley, *Phys. Rev. B* **33**, 2144 (1986).
 - [19] C.-K. Sun *et al.*, *Phys. Rev. B* **50**, 15 337 (1994).
 - [20] R. H. M. Groeneveld, R. Sprik, and A. Lagendijk, *Phys. Rev. B* **51**, 11 433 (1995).
 - [21] M. G. Bawendi *et al.*, *J. Chem. Phys.* **96**, 946 (1992).

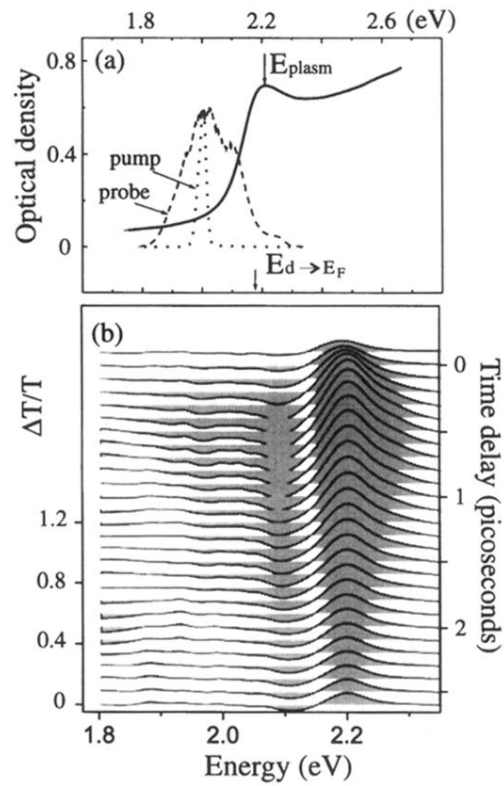


FIG. 1. (a) Absorption spectrum (full line) of the copper nanoparticle sample near the Mie resonance and spectra of the pump (dotted) and probe (dashed) pulses. (b) Pump-probe differential transmittance from the copper nanoparticles with 0.5 mJ/cm^2 pump intensity.